PHYSICAL REVIEW A VOLUME 24, NUMBER 5 NOVEMBER 1981

Electron-impact excitation of hydrogenic ions

N. Abu-Salbi and J. Callaway
Department of Physics and Astronomy, Louisiana State University, Baton Rouge, Louisiana 70803
(Received 22 June 1981)

The $1s \rightarrow 2s$ and $1s \rightarrow 2p$ excitations of the hydrogenic ions C^{5+} and O^{7+} are studied using a pseudostate expansion. A small (3-s, 3-p) basis is used above the $n = 3$ threshold while in the resonance region between the $n = 2$ and $n = 3$ thresholds a larger (6-s, 5-p, 2-d, and 1-f) set is employed. The coupled integrodifferential equations are solved by a variational approach. High-energy and high-L results are found using the Coulomb-Born approximation with exchange. Positions and widths of resonances are given. An analytic fit to the calculated K matrices is used to determine cross sections in the resonance region. Excitation rates are computed.

I. INTRODUCTION

This report describes the application of the variational method to determine electron-impact excitation cross sections of hydrogenic ions using a pseudostate expansion. Procedures are described, and specific applications are made to the ions C^{5+} and O^{7+}. Resonances between the $n=2$ and $n=3$ thresholds are investigated.

The general principles and procedures involved in applications of Kohn-type variational methods to scattering problems in atomic physics are well established. Recent reviews of these methods[1-3] summarize the present situation and contain adequate references to a rather voluminous literature. Most applications have been to hydrogen and helium; in addition, some calculations have been made concerning alkali metals and the atoms C, N, and O. Except for one early application to elastic scattering by He^+,[4] only recently have the procedures been extended to electron ion interactions. In those cases, emphasis has been placed on excitation of He^+,[5-8] where there is a long-standing disagreement between theory and experiment in regard to the energy dependence of the $1s-2s$ cross section.[9] There is also one application to the highly stripped ion Fe^{25+}.[10]

Our decision to consider the specific ions C^{5+} and O^{7+} was motivated in part by their intrinsic importance, and in part by the existence of calculations by other methods, in particular, close coupling[6,11-13] and distorted wave,[13-15] with which our results could be compared. Such comparison is, of course, of great importance in development of a new computational technique. Beyond this, we would like to address two physical questions. (1) How adequate are existing approximation methods in calculating excitation cross sections? (2) What is the effect of resonances between the $n=2$ and $n=3$ thresholds on excitation cross sections and rates.

We will make a few brief introductory comments on each problem. The most significant answer to the question of the accuracy achieved by computational procedures could be furnished by experiment, but measurements on such highly stripped ions do not yet exist. So the most that one can do is to compare results of increasingly more powerful calculations. The most comprehensive calculations for large Z hydrogenic ions which presently exist are generally small basis close-coupling studies, typically three state ($1s$, $2s$, and $2p$) for hydrogenic ions. The question that needs to be investigated is whether three-state close coupling is adequate or more precisely whether the introduction of some pseudostates into the basis set will change cross sections appreciably. It is clear that the addition of pseudostates makes a significant improvement in the intermediate energy range for neutral hydrogen and for He^+.[1,6,7] Presumably the improvement is less striking as the nuclear charge Z increases since general considerations indicate that the relative importance of the electron-electron interaction term decreases with increasing Z. It may be expected that the $2s$ and $2p$ excitation cross sections behave differently in this respect, since the excitation of the $2s$ state involved significant contributions from partial waves of relatively low angular momentum only, whereas in the case of $2p$, large angular momenta are important. Quantitative information concerning the significance of inclusion of pseudostates would be desirable.

There is now a large body of calculations which demonstrate the importance of resonances in the excitation of ions, especially in cases involving transition which are not optically allowed (see, for example, the review by Henry[9]). In contrast to other correlation effects, the importance of resonances does not diminish as Z increases. Seaton points out[16] that in the limit $Z \rightarrow \infty$, resonances acquire a delta-function character and therefore the contribution to excitation rate coefficients from resonances tends to a finite limit relative to the background. At present there

TABLE I. Pseudostate parameters, energies (in Ry), and wave-function coefficients for the 6-state and 14-state bases. Refer to Eq. (1). The $c_{nl,j}$ are arranged in rows according to j in this table. The number given for $c_{nl,j}$ in this table must be multiplied by $Z^{[3/2+m(j)]}$.

	$l=0$		$l=1$	
j	$m(j)$	$\zeta(j)/Z$	$m(j)$	$\zeta(j)/Z$
1	0	1.0	1	1.0
2	0	0.5	1	0.8
3	1	0.5	1	0.5

	$l=0$				$l=1$			
n	E_{n0}/Z^2	$c_{n0,1}$	$c_{n0,2}$	$c_{n0,3}$	E_{n1}/Z^2	$c_{n1,1}$	$c_{n1,2}$	$c_{n1,3}$
1	−1.0	2.0	0.0	0.0	−0.25	0.0	0.204 12	0.0
2	−0.25	0.0	0.707 11	0.353 55	−0.021 45	−3.085 08	−0.568 70	3.619 98
3	0.311 15	7.676 93	−4.858 06	0.809 68	1.125 56	−8.033 35	−0.465 93	5.657 85

	$l=0$		$l=1$		$l=2$		$l=3$	
j	$m(j)$	$\zeta(j)/Z$	$m(j)$	$\zeta(j)/Z$	$m(j)$	$\zeta(j)/Z$	$m(j)$	$\zeta(j)/Z$
1	0	1.0	1	1.0	2	$\frac{1}{3}$	3	0.5
2	0	0.5	1	0.5	2	0.5		
3	1	0.5	1	$\frac{1}{3}$				
4	0	$\frac{1}{3}$	2	$\frac{1}{3}$				
5	1	$\frac{1}{3}$	1	0.2				
6	2	$\frac{1}{3}$						

	$l=0$						
n	E_{n0}/Z^2	$c_{n0,1}$	$c_{n0,2}$	$c_{n0,3}$	$c_{n0,4}$	$c_{n0,5}$	$c_{n0,6}$
1	−1.0	2.0	0.0	0.0	0.0	0.0	0.0
2	−0.25	0.707 11	−0.353 55	0.0	0.0	0.0	0.0
3	−0.111 11	0.384 90	−0.256 60	0.028 51	0.0	0.0	0.0
4	−0.053 75	3.249 00	189.749	16.167 0	−192.575	17.1868	−0.449 46
5	0.117 05	−13.215 3	−345.365	−37.259 7	359.165	−28.7473	0.641 60
6	1.698 18	−34.595 9	−318.335	−41.600 6	348.003	−26.4393	0.555 14

	$l=1$					
n	E_{n1}/Z^2	$c_{n1,1}$	$c_{n1,2}$	$c_{n1,3}$	$c_{n1,4}$	$c_{n1,5}$
1	−0.25	0.0	0.204 12	0.0	0.0	0.0
2	−0.111 11	0.0	0.0	−0.120 96	0.020 16	0.0
3	−0.062 19	0.076 64	−0.438 42	0.350 97	−0.074 52	0.112 19
4	0.027 44	0.908 39	−3.078 14	2.022 13	−0.188 48	0.123 45
5	0.901 92	3.729 59	−3.215 22	1.749 68	−0.137 18	0.070 32

	$l=2$			$l=3$	
n	E_{n2}/Z^2	$c_{n2,1}$	$c_{n2,2}$	E_{n3}/Z^2	$c_{n3,1}$
1	−0.111 11	0.090 17	0.0	0.0	0.004 980 1
2	0.000 65	0.015 68	−0.074 75		

seems to be only one brief report[12] concerning the effect of resonances on scattering in hydrogenic ions with $Z>2$. In that note, results are presented in graphical form only, and a promised publication of rate coefficients had not appeared at the time this article was written. We present below our results concerning resonances in excitation of C^{5+} and O^{7+}.

II. THE PSEUDOSTATE BASIS

The purpose of introducing pseudostates into a close-coupling calculation is to include in some approximate way the contribution of high bound excited states and continuum states while still retaining a basis set of manageable size. This procedure has given cross sections for e-H and e-He^+ excitations which are much improved with respect to those obtained when only a small number of the actual atomic states are included.[1,4,6,7,17,18] The principal difficulty with this procedure is that unphysical pseudoresonances are produced near the (unphysical) thresholds.[19] In previous work, we have avoided this problem by altering the parameters of the pseudostate

basis in order to move the pseudothresholds away from the energy region under investigation.[1] Although this procedure appears to yield satisfactory results, we have decided in this work to investigate the possibility of removing unphysical resonance effects by other methods. Burke *et al.*[20] have recommended averaging the elements of the T matrix by means of a least-squares fit to a low-order polynomial. We have considered this procedure, and an alternative one in which the (pseudo) pole in the K matrix is explicitly identified and removed. These procedures will be discussed below in Sec. V.

The pseudostates are expressed as

$$R_{nl}(r)=\sum_j c_{nl,j} r^{m(j)} \exp[-\zeta(j) r]. \tag{1}$$

Two different sets of pseudostates are used in this work. The first is a small set containing three s-type functions and three p-type functions (exact $1s$, $2s$, and $2p$ states plus three pseudostates) which is employed in the energy range above $n=3$ threshold. It was necessary to restrict the basis set in this way to keep computational time from becoming excessive at high energies where all channels (for any reasonable set) are open. However, although small, this basis has been demonstrated to give quite reasonably good results for He^+.[7] The parameters of this set, and the energies of the states are given in Table I.

The 3-3 basis is not adequate to describe the resonances under the $n=3$ threshold because $n=3$ states are not included. We have therefore used a more extensive basis of six s-type, 5-p, 2-d, and 1-f functions in the range between the $n=2$ and $n=3$ thresholds. This set contains the exact $1s$, $2s$, $3s$, $2p$, $3p$, and $3d$ states plus eight pseudostates. The parameters of this set and the energies of the states are contained in Table I.

It should be noted, in regard to Table I, that we simply scale the pseudostate basis exponents with the nuclear charge Z. Therefore, the energies scale according to Z^2. [Also, note that the energy given pertains to the combination, Eq. (1) rather than to a single element.]

III. THE CALCULATIONAL PROCEDURE

Because differences occasionally arise in the procedures applied here to scattering by ions in comparison with previous work concerning neutral atoms, we believe it is useful to describe briefly the methods employed from the beginning. We start with the two-body Schrödinger equation describing electron scattering by a hydrogenic ion of nuclear charge Z. Atomic units with energies in rydbergs are used.

$$\left(T(1)+T(2)-\frac{2Z}{r_1}-\frac{2Z}{r_2}+\frac{2}{r_{12}}+E\right)\Psi(\vec{r}_1,\vec{r}_2)=0, \tag{2}$$

in which T is the kinetic energy operator and E is the total energy. We shall consider here states characterized by definite values of the total orbital angular momentum L and spin S. Since we are interested only in situations in which an electron is incident on a ground-state ion, the parity is always $(-1)^L$. In addition to these quantum numbers, a channel is described by the pseudostate quantum number n and angular momentum l, the scattering angular momentum l_s, and wave number k. For simplicity, we denote such a collection of indices by a single letter. Thus, in general we write

$$\Psi_a(r_1,r_2)=[1+(-1)^S P_{12}] \times\sum_j G_{ja}(r_2)R_j(r_1)Y_j(\Omega_1\Omega_2), \tag{3}$$

in which j and a are channel indices, Ψ_a contains an incident wave in channel a, and Y_j is a two-body spherical harmonic which is given more explicitly by

$$Y^M_{l_1l_2}(\Omega_1\Omega_2)=\sum_{m_1m_2}(l_1l_2m_1m_2|LM)Y^{m_1}_{l_1}(\Omega_1)Y^{m_2}_{l_2}(\Omega_2), \tag{4}$$

where $(\cdots)$ is a Clebsch-Gordan coefficient and Y^m_l represents an ordinary spherical harmonic. Finally, note that P_{12} in Eq. (3) permutes coordinates (1) and (2).

The function G_{ja} which describes the scattering has the asymptotic form

$$\lim_{r\to\infty} r\,G_{ja}(r)=k_j^{-1/2}(\delta_{aj}\sin\zeta_j+K_{ja}\cos\zeta_j) \qquad (k_j^2>0) \tag{5}$$

$$\lim_{r\to\infty} r\,G_{ja}(r)\sim e^{-|k_j|r} \qquad (k_j^2<0)$$

in which K_{ja} is an element of the symmetric reaction matrix

$$\zeta_j=k_jr-\tfrac{1}{2}l_j\pi+\frac{(Z-1)}{k_j}\ln 2k_jr+\eta_j, \tag{6}$$

and η_j is the Coulomb phase

$$\eta_j=\arg\Gamma(l_j+1-i(Z-1)/k_j). \tag{7}$$

The set of coupled integrodifferential equations satisfied by the functions G_{ja} is derived from the requirement that the two-body Schrödinger equation be satisfied within the subspace spanned by the functions included in the expansion (3). However, we intend to apply a variational method in which the functions G_j are represented by an expansion in terms of known functions

$$G_{ja}(r)=(\alpha_1)_{ja}f_1(l_j,k_j,r)+(\alpha_2)_{ja}f_2(l_j,k_j,r) +\sum_{\nu=1}^{n} b_{ja,\nu}\eta_\nu^{(j)}(r) \quad (k_j^2>0). \tag{8}$$

The objects which appear in (8) are the following. The functions f_1 and f_2 describe the asymptotic form of the wave function in a manner consistent with Eq. (5). If $k_j^2<0$, these terms are absent from Eq. (8). We make the specific choices

$$rf_1(l_j,k_j,r)=k_j^{-1/2}F_{l_j}(k_jr)\,, \tag{9a}$$

$$rf_2(l_j,k_j,r)=k_j^{-1/2}(1-e^{-\gamma r})^{2l_j+1}U_{l_j}(k_j,r)\,. \tag{9b}$$

Here F_{l_j} and U_{l_j} are regular and irregular Coulomb functions which satisfy

$$\left(\frac{d^2}{dr^2}+2\frac{(Z-1)}{r}-\frac{l(l+1)}{r^2}+k^2\right)\begin{pmatrix}F\\U\end{pmatrix}=0 \tag{10}$$

and have asymptotic forms as given in Eq. (5). The multiplicative factor $(1-e^{-\gamma r})^{2l+1}$ in (9b) regularizes U so that $f_2\sim r^l$ as $r\to 0$. The parameter γ is arbitrary, and may be varied at our convenience. (The final results should be stable over a considerable range of γ. We will discuss this in the Appendix.)

The quantities $(\alpha_1)_{ja}$ and $(\alpha_2)_{ja}$ are elements of matrices whose dimensions are $n_0\times n_0$; n_0 being the number of open channels. If $(\alpha_1)_{ja}=\delta_{ja}$, then $(\alpha_2)_{ja}=K_{ja}$; more generally we have[21]

$$K=\alpha_2\alpha_1^{-1}\,. \tag{11}$$

The functions η_ν are square integrable functions which are Slater-type orbitals (STO's), given by

$$\eta_\nu^{(l)}=r^l e^{-\nu r}\,. \tag{12}$$

The same set of exponents ν was used for all channels. Most of the calculations reported here employed a set of 15 ν's. The specific choice depended on the energy range under study. For example, for C^{5+}, calculations with the 3-3 basis up to incident energies three times threshold used a decreasing geometric progression of 15 ν's, the largest being 15.0 and the ratio of successive ν's being 1.3. In general, larger ν's were needed as the energy increased, or as Z increased, and smaller ν's were needed in the resonance region. More details can be found in Ref. 22.

It should be noted that the choice of asymptotic function here differs from both that of our previous work[7,8,10] and from that of Morgan.[5,6] Also an important simplification in comparison with our previous calculations[1,7,8,10] was introduced. In the case of electron scattering by both neutral hydrogen and He^+, it was necessary to introduce energy dependent oscillatory but square integrable functions

$$(1-e^{-\gamma r})^{l+2}\cos k_jr/r^2$$

and

$$(1-e^{-\gamma r})^{l+2}\sin k_jr/r^2$$

into the wave-function expansion. This was done to try to reproduce terms which appear in the asymptotic functions for a channel wave function when the effective Hamiltonian contains long-range off-diagonal coupling terms ($\sim 1/r^2$) connecting channels which are degenerate in energy (as for example the $2s$ and $2p$ states). In this work we are concerned with ions of much larger charge, so that the dipole coupling is relatively less significant. We found that satisfactory accuracy could be obtained when these terms were neglected. This omission significantly reduces calculation time.

Before proceeding to the variational calculations, however, we relate the coefficients $b_{j_a,\nu}$ to the unknown α's. Here, the requirement is that the two-body Schrödinger equation be exactly satisfied within the subspace spanned by the square integrable functions η. Thus, for all channels i and square integrable functions $\eta_\nu^{(i)}$, we have

$$\int \eta_\nu^{(i)}(r_2)R_i(r_1)Y_i^*(\Omega_1\Omega_2)(H-E)\Psi_a(r_1,r_2)d^3r_1d^3r_2=0. \tag{13}$$

When the integrals are carried out, the result is a (large) matrix equation which is solved as discussed, for instance, in Ref. 1. We may then construct the variational functional

$$I_{ab}=\int \Psi_a^*(r_1,r_2)(H-E)\Psi_b(r_1,r_2)d^3r_1d^3r_2\,. \tag{14}$$

This expression is a quadratic form in the matrices α:

$$I_{ab}=\sum_{s,t=1}^{2}\sum_{kl=1}^{n_0}(\alpha_s)_{ka}(\alpha_t)_{lb}\mathfrak{M}_{st}^{kl}\,. \tag{15}$$

The matrix $\mathfrak{M}_{st}^{kl}$ is the characteristic object of variational calculations using Kohn-type methods. We will discuss its computation briefly below. For the moment, we note that standard procedures lead to expressions for the K matrix.[1,2] For example, in the Kohn procedure,

$$K_{ab}=-\mathfrak{M}_{11}^{ab}+\sum_{i,j}\mathfrak{M}_{21}^{ja}(\mathfrak{M}_{22}^{-1})^{ji}\mathfrak{M}_{21}^{ib}\,. \tag{16}$$

We will not consider the specific formulas of this sort that are obtained in different variational procedures as they are discussed in detail in standard references.[1,2]

The numerical work involved in a variational calculation is focused on the calculation of the matrix $\mathfrak{M}$. It has the following form:

$$\mathfrak{M}_{st}^{ni}=F_{st}^{ni}-\sum_{\substack{ij\\ \mu\nu}}M_{s\nu}^{nj}(B^{-1})_{\nu\mu}^{ji}M_{\mu t}^{it}\,, \tag{17}$$

in which

$$F_{st}^{nl}=\int f_s(k_n r_2)R_n(r_1)\,[H_D^{(kl)}(r_1,r_2)+(-1)^S H_X^{(kl)}(r_1,r_2)]\,f_t(k_t r_2)R_t(r_1)r_1^2dr_1r_2^2dr_2 \tag{18}$$

is a free-free integral,

$$M_{s\nu}^{nj}=\int f_s(k_n r_2)R_n(r_1)[H_D^{(nj)}(r_1,r_2)+(-1)^S H_X^{(nj)}(r_1,r_2)]\,\eta_\nu^j(r_2)R_j(r_1)r_1^2dr_1\,r_2^2dr_2 \tag{19}$$

is a bound-free integral, and

$$B_{\mu\nu}^{jt}=\int \eta_\mu^j(r_2)R_j(r_1)\,[H_D^{(j,t)}(r_1,r_2)+(-1)^S H_X^{(jt)}(r_1,r_2)]\,\eta_\nu^t(r_2)R_t(r_1)r_1^2dr_1\,r_2^2dr_2 \tag{20}$$

is a bound-bound integral. The quantities H_D and H_X are given by (in a notation in which l_a, l_b refer to atomic angular momenta and l_i, l_j refer to scattering angular momenta)

$$\begin{aligned}H_D^{(jt)}(r_1,r_2)&=\int d\Omega_1 d\Omega_2 Y^{M*}_{Ll_bl_j}(\Omega_1\Omega_2)(H-E)Y^{M}_{Ll_al_t}(\Omega_1\Omega_2)\\&=\delta_{l_al_b}\delta_{l_tl_j}\left(T_{l_a}(r_1)+T_{l_t}(r_2)-\frac{2Z}{r_1}-\frac{2Z}{r_2}\right)+2\sum_\gamma Q(Ll_bl_jl_al_t\lambda)\frac{r_<^\lambda}{r_>^{\lambda+1}}\end{aligned} \tag{21}$$

and

$$\begin{aligned}H_x^{(jt)}(r_1,r_2)&=\int d\Omega_1 d\Omega_2 Y^{M*}_{Ll_bl_j}(\Omega_1\Omega_2)(H-E)Y^{M}_{Ll_al_t}(\Omega_2\Omega_1)\\&=\delta_{l_bl_t}\delta_{l_al_j}\left(T_{l_b}(r_1)+T_{l_j}(r_2)-\frac{2Z}{r_1}-\frac{2Z}{r_2}\right)+2\sum_\lambda Q(Ll_bl_jl_tl_a\lambda)\frac{r_<^\lambda}{r_>^{\lambda+1}}\,,\end{aligned} \tag{22}$$

in which

$$T_l=-\frac{1}{r^2}\frac{d^2}{dr^2}\left(r^2\frac{d}{dr}\right)+\frac{l(l+1)}{r^2}\,, \tag{23}$$

and the coefficient Q are expressed by

$$\begin{aligned}Q(Ll_bl_jl_al_t\lambda)&=(-1)^{l_a+l_b-L}[(2l_a+1)(2l_b+1)(2l_t+1)(2l_j+1)]^{1/2}\\&\times\begin{Bmatrix}L & l_j & l_b\\ \lambda & l_a & l_t\end{Bmatrix}\begin{pmatrix}l_t & \lambda & l_a\\ 0 & 0 & 0\end{pmatrix}\begin{pmatrix}l_j & \lambda & l_b\\ 0 & 0 & 0\end{pmatrix},\end{aligned} \tag{24}$$

where $\{\cdots\}$ denotes a $6J$ symbol and $(\cdots)$ a $3J$ symbol.

The radial integrals were evaluated by a combination of analytic and numerical techniques. The computation of these types of integrals has been discussed for the case of neutral systems.[23-25] The extension of this work to scattering by ions is described in detail in Ref. 22, which also contains a listing of the computer program employed. The bound-bound matrix could be completely evaluated analytically, but those elements of the bound-free and free-free matrices which involved the irregular Coulomb function had to be evaluated numerically. Shimamura has also considered the analytic evaluation of bound-free integrals for scattering by ions.[26]

The computer programs were checked first for He^+ in the static exchange approximation. Phase shifts in this limit are given by Mott and Massey.[27] We were also able to compare our results with those of Robb[11] in the three-state close-coupling approximation.

IV. FITTING THE K MATRIX

It is not practical to make complete calculations for the closely spaced energies required to permit numerical evaluation of integrals over cross sections in a region containing many resonances. For this reason we have adopted a procedure of making a fit to the K matrix in terms of simple analytic functions. It is then quite practical to calculate cross sections at as many points as are needed. This fitting procedure was developed in previous work on the excitation of C^{3+}.[28] We have also found this method to be useful in regard to the pseudoresonance problem.

Our procedure is based on the work of Eissner and Seaton.[29] The essential point is that the K matrix has a pole in the neighborhood of each reso-

nance. Suppose such a pole occurs at E_λ. Then near E_λ each element of the K matrix for a particular L, S has the form

$$K_{ij}=K_{ij}^{(0)}+C_{ij}/(E_\lambda-E)\,. \tag{25}$$

Furthermore, the residues C_{ij} can be factored

$$C_{ij}=c_i c_j\,. \tag{26}$$

In order to fit our calculated K matrices, we adopt the representation

$$K_{ij}(E)=\sum_{n=0}^{N} D_{ij}^{(n)}(E-E_0)^n+\sum_\lambda \frac{C_{ij}^{(\lambda)}}{E_\lambda-E}\,. \tag{27}$$

The first term on the right of (27) describes the background, which is assumed to be represented as a (low-order) polynomial in energy. The energy E_0 is arbitrary, but is conveniently taken as the lowest energy at which the fit is made. The number of terms in the polynomial is chosen to give a fit of satisfactory accuracy. The second sum in (27) represents the contribution from the resonances.

At first sight, it appears that a nonlinear least-squares calculation, with the attendant convergence problems, would be required to use (27). However, we find that it is quite simple to determine the location of the K-matrix poles E_λ accurately and directly from our *ab initio* calculations. When this is done, the determination of the remaining parameters $D_{ij}^{(n)}$ and $C_{ij}^{(\lambda)}$ is a simple linear least-squares problem. Results based on this procedure are presented in Sec. VII.

V. PULLING THE DRAGON'S TEETH

A major problem associated with the use of pseudostate bases is the existence of unphysical pseudoresonances associated with thresholds for the opening of pseudochannels. If these resonances were narrow, their practical significance would be small; but this is frequently not the case. We describe here the procedure we have used in removing the effects of pseudoresonances (pulling the Dragon's teeth). Other possible pseudothreshold structure appears to be unimportant for our basis.

Burke *et al.*[20] advocate fitting the elements of the T matrix with a low-order polynomial in k by a least-squares method. We experimented with this method and concluded that it is less than optimum unless results are available for a large number of energies rather evenly spaced on both sides of the pseudoresonance. Instead, we choose to work directly with the K matrix. The procedure described in the preceding section is employed in which we first locate the pole in the K matrix and then make a least-squares fit to its elements using

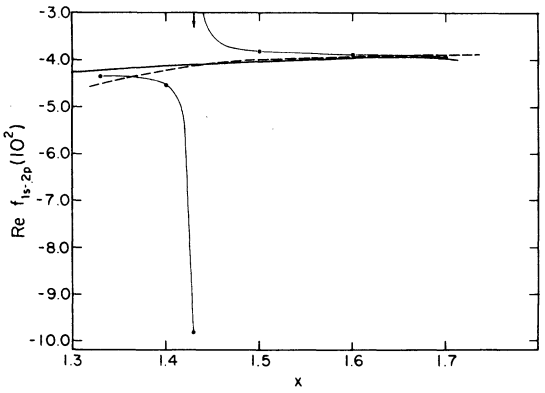

FIG. 1. Real part of the ^1S $1s \rightarrow 2p$ transition amplitude for $e^- - C^{5+}$ scattering is shown as a function of energy (expressed as the ratio of the incident energy to that required to excite the $n=2$ states) in the vicinity of the pseudoresonance at $x=1.431$. The dots (connected by a light solid line as a guide to the eye) are the calculated points. The dashed line is obtained by making a least-squares fit to the amplitude with a quadratic form in k^2; the solid line is the result of the K-matrix fit described in the text.

Eq. (27). The physical K matrix does not have a pole in this energy range so we simply abolish the pole by setting the residues $C_{ij}=0$ and recalculate the cross sections using only the background terms.

An example of this procedure is discussed in connection with Figs. 1, 2, and 3. Our 3-3 basis set has, in the case of e-C^{5+}, a pseudoresonance in the $L=0$ state at approximately $k_i^2=38.6$ Ry associated with the opening of the pseudochannel at 47.2 Ry. This appears to be the only pseudoresonance of significance above the ionization energy. The behavior of the real and the imaginary parts of the transition amplitude for 2-p excitation is shown in Figs. 1 and 2. The rapid variation of this amplitude produces a large variation in the

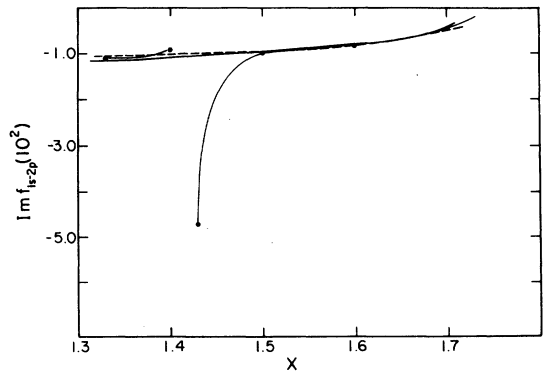

FIG. 2. Same as Fig. 1 except that the imaginary part of the transition amplitude is shown.

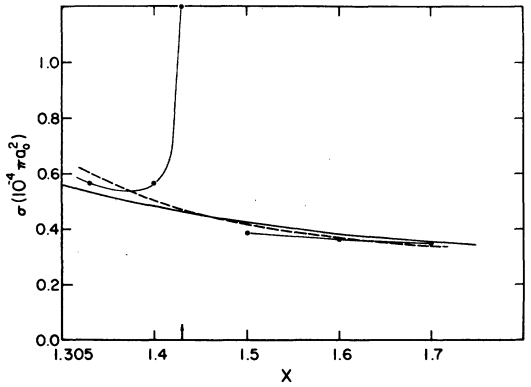

FIG. 3. The $1s \rightarrow 2p$ excitation cross section is shown as computed from the transition amplitude shown in Figs. 1 and 2. Curves have the same significance as in Fig. 1.

excitation cross section, shown in Fig. 3. We examined two ways of removing this spurious structure. In the first, we made a least-squares fit to the amplitude using a quadratic formula

$$f_{1s-2p} = a + bk_i^2 + ck_i^4$$

(the coefficients a, b, c are complex). This procedure produced the results shown by the dashed lines. The procedure in which the K matrix is fit as described above produced results shown by the solid line.

The two methods agree rather well in general. This is particularly true for the imaginary part of the amplitude. There is a tendency for the least-squares fit to the real part to fall (apparently) too low in the low-energy region, and this seems to cause the cross section calculated from this to be too large below the resonance. Probably this would be corrected if the fit were based on more points, symmetrically placed around the pseudoresonance. But when only a relatively small amount of data is available, we think a fit to the K matrix may be preferable.

VI. RESULTS ABOVE THE $n = 3$ THRESHOLD

In this section, the results obtained using the 3-3 basis above the $n = 3$ threshold are discussed.

We determined that the results of variational pseudostate calculations agreed with the (much simpler) results obtained from Coulomb-Born with exchange (CBX) at large L. Above this value of L (called L_{max}) the CBX partial cross sections were used. L_{max} decreases from five near the ionization threshold to two above three times this energy. At still higher energies (>4.5 times ionization) only CBX calculations were made.

Some spin weighted partial cross sections for the $1s$-$2s$ and $1s$-$2p$ transitions in both C^{5+} and O^{7+} are given in Tables II and III. These tables contain only results from the variational calculations except that some CBX contribution is contained in the result presented for the total. It should be noted that the values for $L = 0$, $S = 0$ have been corrected for pseudoresonance structure as described in the preceding section. This is the only partial

TABLE II. Partial and total cross sections for excitation of C^{5+} (units $10^{-4}\pi a_0^2$).

				$1s$-$2s$			
	Singlet			Triplet			
x	$L=0$	$L=1$	$L=2$	$L=0$	$L=1$	$L=2$	Total
1.33	0.502[a]	1.016	0.0112	0.0265	0.368	0.419	2.394
1.50	0.393[a]	0.835	0.0230	0.0324	0.330	0.401	2.090
2.00	0.229	0.536	0.0728	0.0400	0.222	0.314	1.531
2.47	0.148	0.418	0.0847	0.0434	0.203	0.271	1.339
3.33	0.0870	0.227	0.0955	0.0418	0.144	0.195	1.004
4.00	0.0724	0.159	0.0877	0.0450	0.132	0.167	0.905
4.90	0.0491	0.103	0.0803	0.0421	0.109	0.140	0.798
				$1s$-$2p$			
	Singlet			Triplet			
x	$L=0$	$L=1$	$L=2$	$L=0$	$L=1$	$L=2$	Total
1.33	0.534[a]	0.788	3.769	0.0909	0.130	0.320	11.735
1.50	0.420[a]	0.608	2.757	0.107	0.108	0.349	11.315
2.00	0.267	0.282	1.573	0.115	0.0986	0.347	10.932
2.47	0.166	0.192	0.901	0.104	0.0736	0.320	10.364
3.33	0.0958	0.0870	0.419	0.0822	0.0687	0.229	9.469
4.00	0.0648	0.0584	0.266	0.0699	0.0630	0.183	8.892
4.90	0.0380	0.0500	0.154	0.0540	0.0470	0.135	8.202

[a]Corrected for pseudoresonances.

TABLE III. Partial and total cross sections for excitation of O^{7+} (units $10^{-4}\,\pi a_0^2$).

				1s-2s			
	Singlet			Triplet			
x	$L=0$	$L=1$	$L=2$	$L=0$	$L=1$	$L=2$	Total
1.33	0.155[a]	0.352	0.0076	0.0082	0.0974	0.129	0.764
1.56	0.122[a]	0.283	0.0174	0.0119	0.0705	0.113	0.645
2.00	0.0804	0.198	0.0330	0.0174	0.0590	0.0850	0.510
2.45	0.0486	0.139	0.0386	0.0155	0.0545	0.0676	0.425
3.13	0.0343	0.0882	0.0370	0.0153	0.0498	0.0563	0.363
4.00	0.0213	0.045	0.031	0.0140	0.044	0.047	0.289
4.69	0.0160	0.042	0.027	0.0122	0.041	0.052	0.277
				1s-2p			
	Singlet			Triplet			
x	$L=0$	$L=1$	$L=2$	$L=0$	$L=1$	$L=2$	Total
1.33	0.160[a]	0.235	1.211	0.0355	0.0415	0.0989	3.834
1.56	0.125[a]	0.160	0.825	0.0418	0.0467	0.109	3.682
2.00	0.0800	0.0800	0.498	0.0472	0.0360	0.111	3.518
2.45	0.0485	0.0608	0.293	0.0365	0.0346	0.107	3.114
3.13	0.0334	0.039	0.163	0.0281	0.031	0.074	3.058
4.00	0.0186	0.030	0.081	0.0218	0.026	0.041	2.828
4.69	0.0135	0.011	0.056	0.0167	0.012	0.045	2.640

[a]Corrected for pseudoresonances.

wave to show appreciable pseudoresonance effects. Energies are given in terms of the dimensionless ratio of the incident electron energy k_i^2, to the energy required for the excitation of the $n=2$ levels, $\frac{3}{4}Z^2$

$$x = 4k_i^2/3Z^2 . \tag{28}$$

It has become customary to present excitation results for ions in terms of the dimensionless collision strength Ω which is given for the case of hydrogenic ions by

$$\Omega = 2k_i^2\sigma , \tag{29}$$

where σ is the relevant excitation cross section (in units of πa_0^2). In Tables IV and V, we show our results for the collision strengths for the 2s and 2p excitations of C^{5+} and O^{7+}. The value of L_{max} is given, and the contribution from pseudostate and CBX calculations are shown separately. As we have seen in other calculations,[7,10] the excitation of the 2s state is dominated by the low partial waves even at $x \sim 5$; while the optically allowed 2p excitation is dominated by high partial waves at much lower energy. This behavior results from the fact that the effective transition potential is

TABLE IV. Collision strengths for C^{5+}. L_{max} is the maximum L used in pseudostate calculation; CBX stands for Coulomb-Born with exchange. The numbers in parentheses indicate the power of ten by which all numbers in the column are multiplied.

		1s-2s			1s-2p		
x	L_{max}	Ω (ps)	Ω (CBX)	Ω (total)	Ω (ps)	Ω (CBX)	Ω (total)
1.33	5	1.7185(−2)	0.0005(−2)	1.719(−2)	0.666(−1)	0.177(−1)	0.843(−1)
1.50	4	1.692	0.001	1.693	0.460	0.457	0.917
2.00	4	1.640	0.013	1.653	0.821	0.360	1.181
2.47	3	1.700	0.085	1.785	0.549	0.833	1.382
3.33	3	1.637	0.168	1.805	0.396	1.307	1.703
4.00	3	1.717	0.238	1.955	0.345	1.576	1.921
4.90	2	1.385	0.727	2.112	0.126	2.044	2.170
6.06				2.283			2.408
8.17				2.322			2.776
10.00				2.344			3.027
14.84				2.373			3.637

TABLE V. Collision strengths for O^{7+}.

		1s-2s			1s-2p		
x	L_{max}	Ω (ps)	Ω (CBX)	Ω (total)	Ω (ps)	Ω (CBX)	Ω (total)
1.33	5	9.748(−3)	0.002(−3)	9.75(−3)	4.79(−2)	0.109(−2)	4.90(−2)
1.56	4	9.63	0.02	9.65	4.64	0.874	5.51
2.00	4	9.74	0.06	9.80	4.67	2.09	6.76
2.45	3	9.54	0.46	10.0	2.90	4.42	7.32
3.13	3	10.1	0.83	10.9	2.26	6.93	9.19
4.00	2	7.76	3.34	11.1	0.861	10.0	10.9
4.69	0	1.27	11.2	12.5	0.136	11.8	11.9
5.33				12.7			12.8
9.80				13.2			17.1

short ranged in the case of the 2s state, long ranged for 2p. It is just this property of sensitivity to low partial waves which makes the results for the 2s cross section somewhat sensitive to the basis employed.

For the convenience of potential users of this data, we have fit the collision strength for $x \geq 1.33$ by the analytic formula

$$\Omega(x) = a \ln x + b + \frac{c}{x} + \frac{d}{x^2} . \tag{30}$$

(However, $a = 0$ for the 2s excitation.) The coefficients are given in Table VI. The fits for C^{5+} are accurate to better than 1% for the 2p excitation, but are not so accurate (extreme case is a 5% error) for the 2s. Adding another term ($\sim 1/x^3$) does not make a significant improvement. The fit for the 2s transition in O^{7+} is of similar accuracy (extreme error ~4%), while for the 2p excitation of O^{7+}, the fit to the 2p has an extreme-case error of 4%.

Inspection of the data of Tables IV and V reveals some fluctuations in the computed collision strength at the few percent level which results from an imperfectly smooth transition between the pseudostate and CBX calculations. These fluctuations are smoothed by the least-squares fit and we recommend use of these formulas in applications of our results.

TABLE VI. Coefficients in the fit to the collision strengths, Eq. (30).

	C^{5+}		O^{7+}	
Coef	1s-2s	1s-2p	1s-2s	1s-2p
a		0.1259		0.0730
b	0.0273	0.0104	0.0152	0.00398
c	−0.0378	0.0172	−0.0181	−0.000566
d	0.0327	0.0437	0.0145	0.0446

We have compared our results in this energy range with other calculations in Figs. 4–7. We discuss the 2s excitation first. In both C^{5+} and O^{7+} our collision strengths have a different shape as well as being smaller at low energies than is found in other work. We obtain a minimum in the collision strength for x slightly smaller than two. Pseudostate calculations for the 2s excitation in H^1 and He^{+7} also show a minimum in the neighborhood of $x = 2$. Our value for the collision strength in C^{5+} at $x = 2$ is smaller than is obtained in the three-state close-coupling (3CC) calculation of Hayes and Seaton[13] by 14%. The inclusion of pseudostates does make a meaningful difference in this case. Morgan also observed that use of pseudostates lead to a 10–15% reduction of this cross section in the energy region close to the $n = 2$ threshold.[6] It should be mentioned that there is a shallow minimum in $\Omega(x)$ in the 3CC calculation at

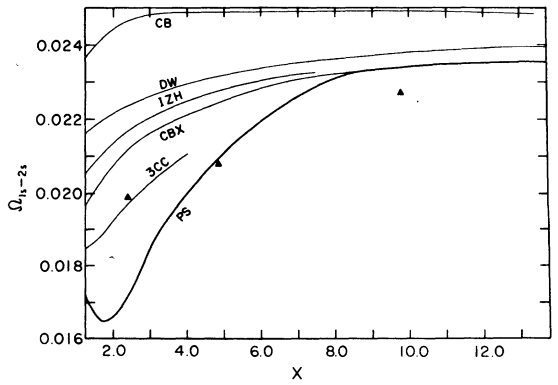

FIG. 4. Collision strength for 2s excitation of C^{5+}. Curves are ps, present pseudostate calculation [from Eq. (30) with coefficients in Table VI], 3CC, three-state close coupling, CBX, Coulomb-Born exchange, IZH, infinite Z hydrogenic, DW, distorted wave, CB, Coulomb-Born. The triangles are the results of Ref. 32.

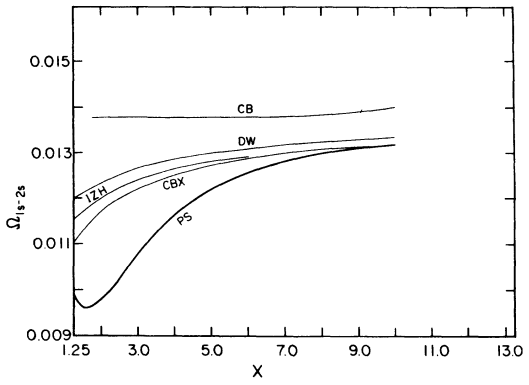

FIG. 5. Collision strength for $2s$ excitation of O^{7+}.

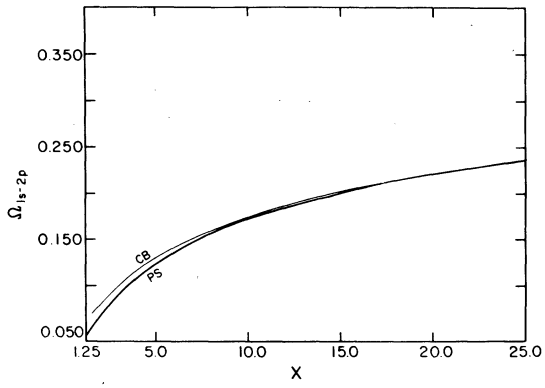

FIG. 7. Collision strength for $2p$ excitation of O^{7+}.

a lower energy than is shown on this graph; that is, in a range where resonance effects neglected by 3CC are important. (Our results in the resonance region are discussed in the next section.)

Other calculations which yield larger collision strengths at low energies include Coulomb-Born exchange (CBX), the infinite-Z hydrogenic method (IZH) (Ref. 30), and distorted wave (DW). The DW values shown on the graph are those of Mann[14]; somewhat lower values, rather close to IZH are found by Baluja and McDowell.[15] Because of the widespread use of DW calculations for stripped ions, it is useful to note that for C^{5+} our result at $x = 2$ is almost 29% below DW.[14] This may be large enough to be of practical significance. Coulomb-Born without exchange[31,14] (CB) results are yet substantially larger. A few points are available from a second-order potential calculation.[32]

Calculations by other methods for the $2p$ excitation yield results which are almost indistinguishable from ours on the scale of the graphs of Figs. 6 and 7 except for Coulomb-Born. Our values are about 11% lower than 3CC at $x = 1.33$, but the difference is reduced to about 3% by $x = 2$. Morgan also found a significant reduction in the $2p$ excitation cross section near the $n = 2$ threshold.[6] Also, DW works well above about $x = 2$. It is probable that the greater effect of inclusion of pseudostates and of a more complicated calculational method on the $2s$ cross section is a consequence of the short-range nature of the transition potential for that state, as mentioned in the Introduction.

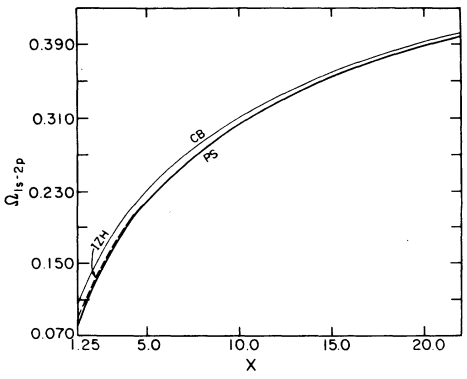

FIG. 6. Collision strength for $2p$ excitation of C^{5+}.

VII. RESULTS: THE RESONANCE REGION

There are infinite series of resonances under each excitation threshold in hydrogenic ions. The variational method seems to be well adapted to determining the positions and widths of these states. We report here our results for resonances between the $n = 2$ and $n = 3$ thresholds. We have found resonances in all partial waves from ^1S through ^3G.

This calculation was based on the 6-5-2-1 pseudostate basis whose parameters are listed in Table I. Our values for positions and widths were determined by fitting the calculated eigenphase sum η_T to the formula

$$\eta_T = \eta_B + \tan^{-1}[\Gamma/2(E_0 - E)] , \tag{31}$$

in which E_0 is the position of the resonances, Γ is the width, and η_B represents the background. Our values for the positions and widths are presented in Table VII, where they are compared with values obtained by Ho[33] who employed the complex rotation method with a basis of Hylleras-type functions. We are not aware of other numerical results for these values of Z (Hayes and Seaton[11] give results in graphical form only).

In the first place, the agreement between the present scattering calculation and those of the complex rotation method is good in those cases for which results of both types of calculations exist. We have located many additional resonances in this work.[34] Our procedures are not as efficient as the complex rotation method is for finding

TABLE VII. Energies and widths of scattering resonances between the $n=2$ and $n=3$ thresholds for $Z=6$ and $Z=8$. Energies are measured in terms of the scaled variable x [Eq. (28)]; widths are in Rydbergs. Rows labeled a are the present results, rows labeled b contain the results of Ho (Ref. 33).

	^1S		^3S		^1P		^3P		^1D	
	x_{12}	Γ	x_{12}	Γ	x_{12}	Γ	x_{12}	Γ	x_{12}	Γ
					$Z=6$					
a	1.058 32	0.0095	1.115 754	0.000 097	1.063 73	0.0286	1.059 08	0.0075	1.061 29	0.0129
b	1.058 32	0.0095			1.063 69	0.0280	1.059 08	0.0074		
a	1.069 49	0.0385	1.120 529	0.000 34	1.081 60	0.0081	1.070 57	0.003 07	1.068 94	0.0226
b	1.069 45	0.0386			1.081 17	0.0078	1.070 49	0.003 08		
a					1.121 16	0.0171	1.118 16	0.0041	1.078 89	0.0080
b	1.089 52	0.000 57								
a	1.117 75	0.0060			1.130 56	0.0037	1.124 93	0.0012	1.119 38	0.0068
b	1.117 73	0.0060								
a	1.124 92	0.0203							1.124 14	0.0125
b	1.124 72	0.0196								
					$Z=8$					
a	1.053 11	0.0100	1.112 344	0.000 11	1.057 30	0.0308	1.053 68	0.0077	1.055 36	0.0132
b	1.053 11	0.0100			1.057 27	0.0306	1.053 68	0.0075		
a	1.061 85	0.0426	1.116 004	0.000 38	1.071 44	0.0089	1.062 52	0.003 19	1.061 29	0.0250
b	1.061 80	0.0418			1.071 14	0.0087	1.062 47	0.003 16		
a					1.116 54	0.0200	1.114 19	0.0036	1.069 26	0.0090
b	1.077 54	0.000 51								
a	1.113 88	0.0070			1.124 24	0.0041	1.119 48	0.0013	1.115 18	0.0082
b	1.113 88	0.0066								
a	1.119 58	0.0230							1.118 88	0.0139
b	1.119 45	0.0224								

	^3D		^1F		^3F		^1G		^3G	
	x_{12}	Γ	x_{12}	Γ	x_{12}	Γ	x_{12}	Γ	x_{12}	
					$Z=6$					
a	1.066 07	0.0019	1.074 21	0.024	1.064 57	0.000 065	1.073 48	0.047	1.124 27	0.000 87
a			1.123 72	0.0027			1.124 39	0.0199		
a			1.126 89	0.0110			1.128 91	0.0042		
					$Z=8$					
a	1.059 075	0.0020	1.065 64	0.0279	1.057 923	0.000 093	1.065 01	0.054	1.118 93	0.000 96
a			1,118 48	0.0029			1.119 03	0.0221		
a			1.121 20	0.0136			1.123 01	0.0061		

very narrow resonances, and we have not obtained the third ^1S resonance. Possibly it has a dominant configuration not representable in our basis. It is worth noting that many of the resonances have widths equivalent to 0.5 eV or greater. In addition, most of the resonances have widths which increase gradually with Z.

The K-matrix fitting technique described in Sec. IV was used to study the cross section in the resonance region. An example of this is shown in Fig. 8, which illustrates the ^1P contribution to the $1s$-$2s$ cross section in C^{5+}. In this case calculations were made at 36 energies between $x=1.01$ and $x=1.16$ and the K-matrix fit was used to obtain results at 1851 energies (on a grid with $\Delta x = 0.0001$). We believe this is sufficient to enable

TABLE VIII. Thermally averaged excitation cross section for C^{5+} (units $10^{-4}\,\pi a_0^2$) are given at selected electron temperatures (in eV).

T (eV)	$\sigma_{1s\text{-}2s}(10^{-4}\,\pi a_0^2)$	$\sigma_{1s\text{-}2p}(10^{-4}\,\pi a_0^2)$
50	0.0161	0.0680
100	0.311	1.432
150	0.695	3.478
200	0.954	5.142
250	1.101	6.312
500	1.174	8.264
750	1.033	8.207
1000	0.901	7.780
1250	0.796	7.328
1500	0.712	6.877
1750	0.644	6.482
2000	0.588	6.137

the calculation of the resonant contribution to rate coefficients by straightforward numerical integration.

Our results for the total cross sections in the resonance region are shown for both C^{5+} and O^{7+} in Figs. 9–12. It will be seen that the resonances fall clearly into two groups separated by about 1 Ry in C^{5+} and 2 Ry in O^{7+}. The resonances in the lower group may be roughly described as $(3l, 3l')$; one electron in an $n=3$ state of angular momenta l in the original ion; the other electron bound in a state with $n=3$, angular momentum l', in the field of an ion of charge $Z-1$. The upper group are the $(3l, 4l')$ resonances. Obviously there are higher groups of resonances that we have not studied. Studies of the graphs indicates qualitatively (and this is confirmed by the quantitative results presented in the next section) that the resonant enhancement of the calculated rate coefficients will not be large. Even though the individual resonances are quite narrow, the structure of the $(3l, 3l')$ extends over a substantial energy range: ~9 eV in the case of C^{5+}, 12 eV in O^{7+}, so that some

TABLE IX. Thermally averaged cross sections for O^{7+}.

T (eV)	$\sigma_{1s\text{-}2s}(10^{-4}\,\pi a_0^2)$	$\sigma_{1s\text{-}2p}(10^{-4}\,\pi a_0^2)$
100	0.0107	0.0463
150	0.0618	0.280
200	0.1358	0.644
250	0.207	1.023
500	0.378	2.21
750	0.394	2.58
1000	0.374	2.66
1250	0.347	2.64
1500	0.320	2.57
1750	0.297	2.49
2000	0.276	2.41

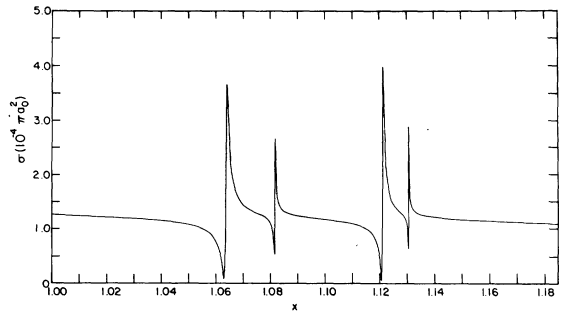

FIG. 8. The ^1P contribution to the $2s$ excitation of C^{5+} is shown in the resonance region.

observation of these resonant groups may be possible, provided suitable ionic beams can be prepared.

VIII. THERMAL AVERAGES

We have used the preceding results for the energy dependence of excitation cross sections to calculate the thermal average cross section. This quantity is closely related to the excitation rate, and is defined by

$$\sigma_e = \frac{1}{V_A}\int P(v)v\sigma(v)dv\,, \tag{32}$$

in which $P(v)$ is the Maxwellian velocity distribution and v_A is the average thermal velocity. Let the electron temperature be denoted by Θ. Then

$$v_A = (8K\Theta/\pi m)^{1/2},$$

in which K is Boltzmann's constant and m is the electron mass. In terms of the variable x introduced previously, we have

$$\sigma_e = q^2\int_1^\infty xe^{-\alpha x}\sigma(x)dx$$

$$= \frac{q}{2K\Theta}\int_1^\infty e^{-\alpha x}\Omega(x)dx\,, \tag{33}$$

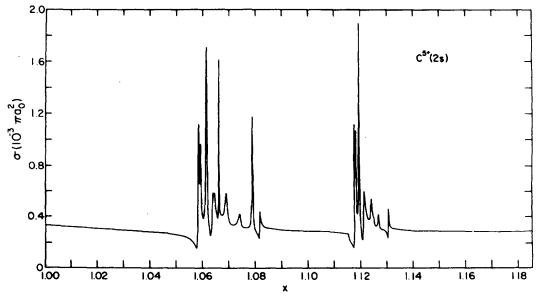

FIG. 9. The cross section for the $2s$ excitation of C^{5+} (units $10^{-4}\,\pi a_0^2$) in the resonance region is shown as a function of the dimensionless energy ratio x, Eq. (28).

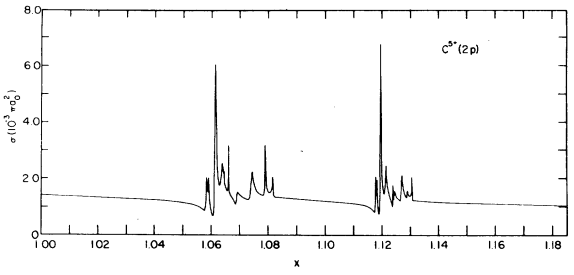

FIG. 10. Cross section for the $2p$ excitation of C^{5+} (units $10^{-3}\ \pi a_0^2$) in the resonance region.

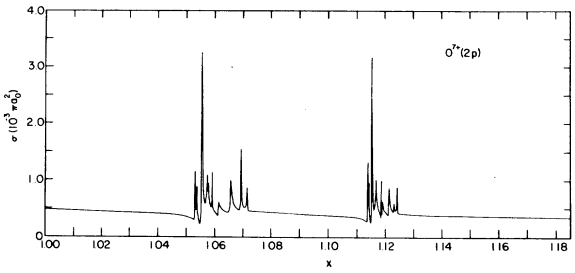

FIG. 12. $2p$ excitation cross section for O^{7+}.

in which

$$q = E_x/K\Theta$$

and E_x is the excitation energy.

The conventional rate coefficient R (in units $\mathrm{cm^3\,sec^{-1}}$) is given by (see Magee *et al.*, Ref. 11)

$$R = c(K\Theta)^{1/2}\sigma_e ,$$

where σ_e is in units of πa_0^2 and $c = 8.010 \times 10^{-8}$ when $K\Theta$ is given in electron volts.

The region of integration has been broken into two parts in order that we may include the contribution of resonances. In the low-energy region $x < x_0 = 1.1852$ (the position of the $n=3$ threshold), we use the cross sections obtained from the K-matrix fit to the results of the 6-5-2-1 basis. The fitting procedure makes possible rapid evaluation of the cross section at enough points to permit straightforward numerical evaluation of the integral. For $x > x_0$, we use the empirical fit to the collision strength given by Eq. (30). The contribution from this region to the average cross section is given by

$$\frac{q}{2K\Theta}\int_{x_0}^{\infty}\Omega(x)e^{-qx}dx = \frac{1}{2K\Theta}\left[\left(a\ln x_0 + b + \frac{dq}{x_0}\right)e^{-qx_0} + (a + cq - dq^2)E_1(qx_0)\right], \tag{34}$$

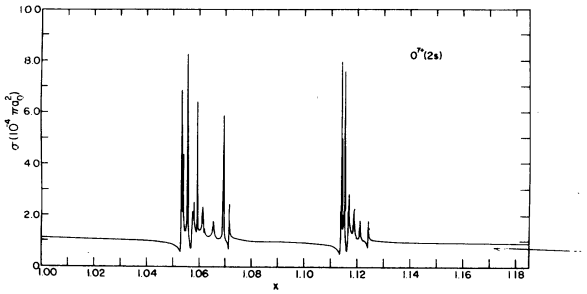

FIG. 11. $2s$ excitation cross section of O^{7+}.

in which E_1 is an exponential integral function.

Our results for the thermal averaged cross sections are presented in Tables VIII and IX, and are shown graphically in Figs. 13 and 14. We have compared our results with those obtained by fitting the results of the distorted-wave calculations of Mann[14] with the empirical representation (30). Our averages for the $2s$ cross sections are significantly below those of Mann, by more than 20% near the maximum of the rate curve in the case of C^{5+} and by slightly less than 20% for O^{7+}. In the case of the $2p$ transition, the difference is rather insignificant (<1% above $T = 1$ keV) except at the lowest energies listed, where our values are more than 5% lower than those of Mann.

The net effect of inclusion of resonances was investigated by repeating the calculations of thermal average cross sections neglecting the resonances, that is, considering only the background cross section. In fact, the resonant enhancement of the

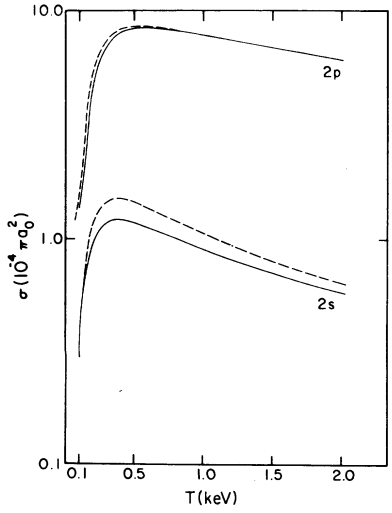

FIG. 13. Thermal average cross sections for the $2s$ and $2p$ excitations of C^{5+} (units $10^{-4}\ \pi a_0^2$) are given as a function of electron temperature in keV. The solid curves represent the present results. The dashed curves are based on the distorted-wave calculation of Mann (Ref. 14).

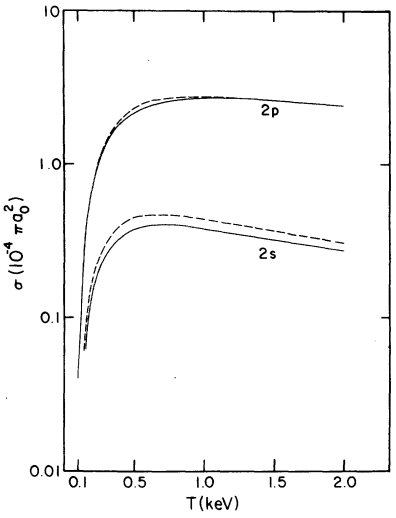

FIG. 14. Thermal average cross sections for the $2s$ and $2p$ excitation of O^{7+}. Curves are drawn as in Fig. 13.

thermal average cross section is quite small, for both the $2s$ and $2p$ cases (~1% or less for $T > 750$ eV). At the lowest temperature studied there is about a 6% resonant enhancement of the average $2s$ cross section, and about 3% for the $2p$. Inclusion of higher resonances would probably increase this only slightly.

Finally, it should be noted that the calculations of cross sections in the resonance region with the 6-5-2-1 basis show a lower background (by perhaps 10% for the $2s$) than do the results from the $3s$-$3p$ basis in the same range. We find that if the thermal average is calculated using the 3-3 basis in Eq. (34) with $x_0 = 1$, the results agree rather well with those of the more elaborate procedure previously described. The errors of the

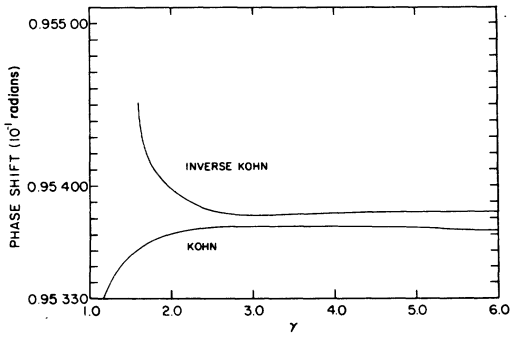

FIG. 15. The ^1S phase shift for elastic scattering of electrons by C^{5+} in the static exchange approximation at an incident energy of 16 Ry is shown as a function of the parameter γ [Eq. (9b)] according to both the Kohn and inverse Kohn methods.

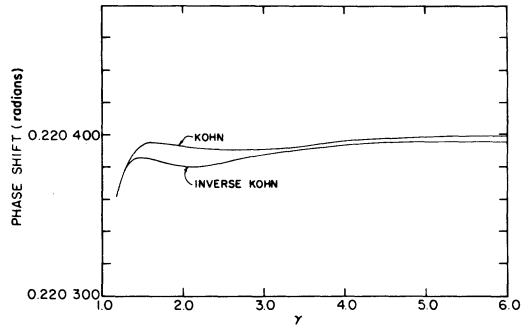

FIG. 16. Same as Fig. 17 but for the ^3S phase shift.

3-3 basis: neglect of resonances and too large background cancel to a substantial extent. Therefore potential users of these results will be justified in using the simpler procedure.

IX. CONCLUSIONS

Calculations of cross sections and excitation rates for C^{5+} and O^{7+} including pseudostates show a significant decrease (~20%) for the $2s$ transition in comparison to the quick and popular distorted-wave method. However, the reduction of the $2p$ excitation cross section is much smaller, and probably of little practical importance. Numerous resonances have been predicted but their net effect on rate coefficients is small. Adequate results for rate coefficients can therefore be obtained from the use of a simple formula based on a semiempirical representation of the collision strength.

APPENDIX: DETERMINATION OF THE PARAMETER γ

This parameter appears in the regularizing factor of the irregular Coulomb function, Eq. (9b). It would be desirable to run complete sets of excitation calculations for different values of γ in order to check stability with respect to variation of γ, but this would require an unrealistically large expenditure of computer time. We have therefore chosen a simpler problem for this experimentation: elastic scattering in the static exchange approximation. The results are interesting enough to deserve brief mention in this paper.

Figures 15 and 16 show the elastic s-wave phase shift; for singlet and triplet spin states for C^{5+} at an incident energy of 16 Ry. The calculations were carried out using a set of 13 short-range functions, whose exponents ν [see Eq. (12)] were in a geometric progression with maximum value 15.6 and decreased in a ratio of 1.3. It is seen that a very reasonable range of stability is obtained over a large range of γ (the phase shift varies only in the

fifth and sixth decimal places). Based on this evidence, we used $\gamma = 3.6$ for C^{5+} in most of our calculations. Similar results for O^{7+} lead to a choice of $\gamma = 4.8$ for that element, e.g., γ scales approximately with Z.

[1]J. Callaway, Phys. Rep. 45, 89 (1978).
[2]R. K. Nesbet, *Variational Methods in Electron-Atom Scattering Theory* (Plenum, New York, 1980).
[3]D. G. Truhlar, J. Abdallah, and R. L. Smith, Adv. Chem. Phys. 25, 211 (1974).
[4]B. H. Bransden and A. Dalgarno, Proc. Phys. Soc. London Sect. A 66, 268 (1953).
[5]L. A. Morgan, J. Phys. B 12, L735 (1979).
[6]L. A. Morgan, J. Phys. B 13, 3703 (1980).
[7]S. A. Wakid and J. Callaway, J. Phys. B 13, L605 (1980).
[8]S. Wakid and J. Callaway, Phys. Lett. 78A, 137 (1980).
[9]R. J. W. Henry, Phys. Rep. 68, 1 (1981).
[10]S. A. Wakid and J. Callaway, Phys. Lett. 81A, 333 (1981).
[11]W. D. Robb, quoted by N. H. Magee, J. B. Mann, A. L. Merts, and W. D. Robb, Los Alamos Scientific Laboratory Report No. LA-6991-MS, Los Alamos, New Mexico (unpublished).
[12]M. A. Hayes and M. J. Seaton, J. Phys. B 11, L79 (1978).
[13]M. A. Hayes and M. J. Seaton, J. Phys. B 10, L573 (1977).
[14]J. B. Mann, quoted in Ref. 11, and private communication.
[15]K. L. Baluja and M. R. C. McDowell, J. Phys. B 10, L673 (1977).
[16]M. J. Seaton, J. Phys. B 2, 5 (1969).
[17]P. G. Burke and T. G. Webb, J. Phys. B 3, L131 (1970).
[18]R. J. W. Henry and J. J. Matese, Phys. Rev. A 14, 1368 (1976).
[19]P. G. Burke and J. F. B. Mitchell, J. Phys. B 6, 320 (1973).
[20]P. G. Burke, K. A. Berrington, and C. V. Sukumar, J. Phys. B 14, 289 (1981).
[21]M. J. Seaton, Proc. Phys. Soc. London 89, 469 (1966).
[22]N. Abu-Salbi, Ph.D. thesis, Louisiana State University, 1981 (unpublished); available from University Microfilms International, Ann Arbor, Michigan, 48106.
[23]J. D. Lyons and R. K. Nesbet, J. Comput. Phys. 4, 499 (1969); 11, 166 (1973).
[24]F. E. Harris and H. H. Michels, J. Comput. Phys. 4, 579 (1969).
[25]R. S. Oberoi, J. Callaway, and G. J. Seiler, J. Comput. Phys. 10, 466 (1972).
[26]I. Shimamura, J. Phys. Soc. Jpn. 31, 217 (1971).
[27]N. F. Mott and H. S. W. Massey, *The Theory of Atomic Collisions*, 3rd ed. (Oxford University Press, Oxford, 1965), p. 559.
[28]J. Callaway, J. N. Gau, R. J. W. Henry, D. H. Oza, Vo Ky Lan, and M. LeDourneuf, Phys. Rev. A 16, 2533 (1977).
[29]W. Eissner and M. J. Seaton, J. Phys. B 7, 2523 (1974).
[30]D. H. Sampson, Astrophys. J. Suppl. 28, 309 (1974) and as quoted by Magee *et al.*, Ref. 11.
[31]J. A. Tully, Can. J. Phys. 51, 2047 (1973), and as quoted by Magee *et al.*, Ref. 11.
[32]B. H. Bransden and C. J. Noble, J. Phys. B 9, 1507 (1976); and as quoted by Magee *et al.*, Ref. 11.
[33]Y. K. Ho, J. Phys. B 12, 387 (1979).
[34]Y. K. Ho and J. Callaway (unpublished), will report positions and widths of high-angular-momentum resonances obtained from the complex rotation method with a different basis.